ADVANCED MATERIALS
www.advmat.de

Plant-Like Tropisms in Artificial Muscles

Shazed Aziz, Xi Zhang, Sina Naficy, Bidita Salahuddin, Edwin W. H. Jager, and Zhonghua Zhu**

Helical plants have the ability of tropisms to respond to natural stimuli, and biomimicry of such helical shapes into artificial muscles has been vastly popular. However, the shape-mimicked actuators only respond to artificially provided stimulus, they are not adaptive to variable natural conditions, thus being unsuitable for real-life applications where on-demand, autonomous operations are required. Novel artificial muscles made of hierarchically patterned helically wound yarns that are self-adaptive to environmental humidity and temperature changes are demonstrated here. Unlike shape-mimicked artificial muscles, a unique microstructural biomimicking approach is adopted, where the muscle yarns can effectively replicate the hydrotropism and thermotropism of helical plants to their microfibril level using plant-like microstructural memories. Large strokes, with rapid movement, are obtained when the individual microfilament of yarn is inlaid with hydrogel and further twisted into a coil-shaped hierarchical structure. The developed artificial muscle provides an average actuation speed of ≈5.2% s^{-1} at expansion and ≈3.1% s^{-1} at contraction cycles, being the fastest amongst previously demonstrated actuators of similar type. It is demonstrated that these muscle yarns can autonomously close a window in wet climates. The building block yarns are washable without any material degradation, making them suitable for smart, reusable textile and soft robotic devices.

1. Introduction

The concept of developing artificial muscles by synthesizing and/or configuring smart materials and structures has come from assemblies of living systems, known as biomimicking, such as mimicking the shape of different animals and plants.[1] Inspiration from plants is adopted for the reason that they are composed of safe and abundant cellulose polymers, and use variations of natural stimuli to trigger autonomous movements known as plant tropisms, for instance to follow the sun or catch an insect.[2] While the energy conversion efficiency of artificially stimulated muscles is very low, naturally triggered muscles have no such limitations and provide environmentally friendly, autonomous operation strategies.[3] Thus far scientists have achieved biomimicking only of the shape of natural creatures when developing artificial muscles.[4] Shape-mimicking approaches have limitations of being irrecoverable, hysteretic, thus not adaptive to a constantly changing environment, preventing artificial muscles from commercial usage.[5] Microstructure mimicking of plant tropisms can overcome these limitations and make the artificial muscles naturally intelligent and adaptive to variable environments. Unfortunately, to the best of our knowledge, the study of mimicking plant-like tropisms in artificial muscles has never been conducted. We therefore develop self-adaptive artificial muscle that distinctly mimics the hydrotropism and thermotropism of helical plants. Practically, self-adaptive artificial muscles reveal an ever-expanding range of applications in automated technologies including disaster response, autonomous surveying, and sensitive prosthetics.

In plants with tropism features, helical configurations are common which enable their stimuli responsiveness to be greater than those with linear shapes. Most of these helical plants have a hierarchy of microstructural chirality with the helices of cellulose fibrils, and upon moisture and heat-induced volume change, these fibrils produce torsion that eventually triggers uniaxial length change of the overall system. Helical plant tendrils are excellent inspiration for developing artificial muscles (**Figure 1**) as they exhibit a combination of hydrotropism and thermotropism, that is, humidity and heat-driven volume expansion/contraction, through the helix that changes the angle of cellulose microfibrils at the subcellular level, leading to a linear length change through the tendril axis direction (Figure 1A).[6] Although nanocarbon

S. Aziz, X. Zhang, B. Salahuddin, Z. Zhu
School of Chemical Engineering
The University of Queensland
St Lucia, QLD 4072, Australia
E-mail: b.salahuddin@uq.edu.au; z.zhu@uq.edu.au
S. Naficy
School of Chemical and Biomolecular Engineering
The University of Sydney
Sydney, NSW 2006, Australia
E. W. H. Jager
Division of Sensor and Actuator Systems
Department of Physics, Chemistry, and Biology (IFM)
Linköping University
Linköping SE-58183, Sweden
E-mail: edwin.jager@liu.se

The ORCID identification number(s) for the author(s) of this article can be found under https://doi.org/10.1002/adma.202212046

DOI: 10.1002/adma.202212046

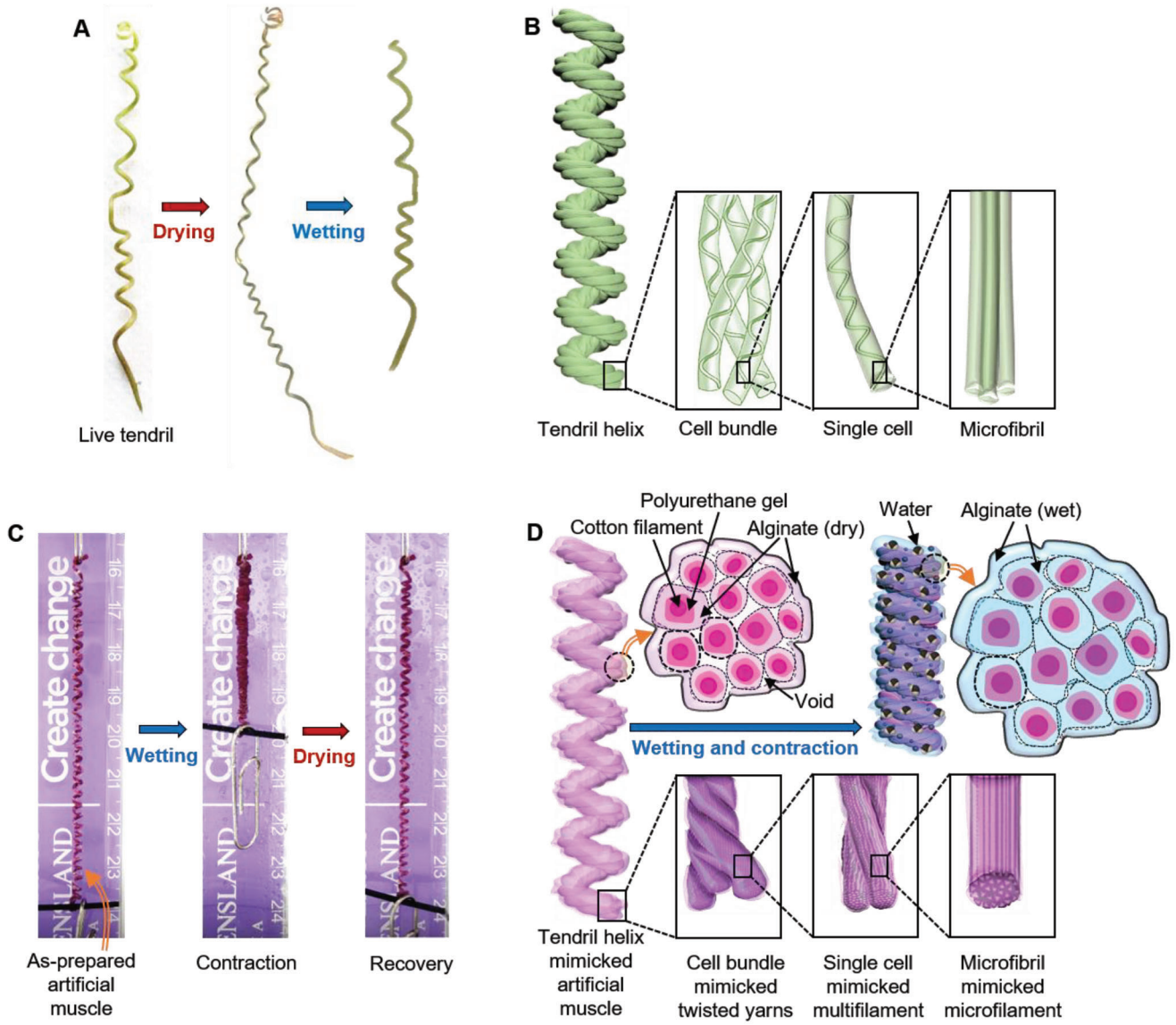

Figure 1. Summary work on the microstructural mimicking of helical plant tendrils for making moisture-responsive artificial muscles. A) A live plant tendril* with large intercoil spacing provides large linear expansion and contraction upon drying and wetting, respectively. B) Schematic illustration of the hierarchy of a plant tendril with macro- and microscopic components. C) A plant tendril mimicked coiled artificial muscle provides large linear contraction and expansion (≈50% of the initial length) upon wetting and drying, respectively. D) Schematic illustration of the microstructural mimicking of a plant tendril to make a coiled artificial muscle with the capability of high contractile actuation and the underlying mechanism of moisture-driven actuation. *Live tendrils were sourced from the Plants Store of Bunnings Group Limited, Australia. Drying and wetting of the tendrils were performed under normal environment.

materials such as carbon nanotube yarns and graphene yarns have been popular in making moisture-driven helical muscles,[7] they are still expensive, not suitable for high-volume production, and rather hazardous to the environment and the users. Many researchers also used readily available natural and synthetic polymer yarns; however, these systems are not energy efficient. Most of the research on helical plant-inspired polymer yarn artificial systems used external energies through thermal,[2b,8] electrical,[9] chemical,[2a,8b] radiation,[10] or electrochemical processes[11] for either muscle fabrication and/or triggering actuation. In regards to the practical utilities of artificial muscles, it is essential for them to have the ability to adapt to their surrounding environments to work effectively in variable natural conditions. Evolutionary actuators, for example, polymer coil muscles, intend to address this by shape manipulation in controlled laboratory environments.[12] However, it is practically impossible to replicate the abundance of natural interactions in a controlled and artificial environment. A combination of mimicking fundamental natural phenomenon, for example, plant tropisms, in artificial muscles and their activation via naturally found stimuli can solve their long persistent limitations, resulting in artificial muscles with controlled performance and environmental adaptiveness.

While mimicking tropisms, it is also essential to design artificial muscles that effectively produce high and fast actuation strokes. It is therefore required to have helices with substantial intercoil spacings as these spaces are to accommodate linear actuation strain when moisture is diffused. For instance, the large intercoil spacing of a tendril allows for high liner actuation strain in the helical configuration (Figure 1A). Helical tendrils have a hierarchy of chirality consisting of microscopic cellulose molecules, microfibrils, single cells, and cell bundles within the macroscopic tendril helix (Figure 1B).[13] The helix direction for all components is identical (producing a homochiral structure), and the moisture-induced volume change produces torsion along the helix direction, eventually resulting in uniaxial length contraction. We here mimic the macro- and microscale homochiral structures (tendril helix, cell bundle, single cell, and microfibril) of tendrils in our coiled artificial muscles (Figure 1D). Yarns consisting of hundreds of microfilaments (mimicking cellulose microfibrils) could be useful for this purpose as they can be configured into hierarchical microstructure as found in tendrils, using textile processing techniques including blending, mixing, or stapling. As these yarns comprise a variety of multiscale internal spaces, infusing a hygroscopic material, such as hydrogel, into these spaces followed by highly twisting makes these yarns similarly structured to tendril filaments that contain a single cell (Figure 1C). Incorporation of hydrogel within the yarn would enable efficient moisture diffusion within the multifilament yarn, providing volumetric expansion to this single-cell mimicked yarn resulting in torsional rotation (untwisting) to the co-twisted cellulose microfibrils. Further twisting the multifilament yarn would form a coiled actuator; however, such coils will be of high compactness with low linear actuation capabilities.[14] We therefore applied a mandrel-based coiling technique (wrapping the highly twisted yarn around a metal shaft) that forms the desired coiled actuator (Figure 1C) whose shape is similar to a macroscale tendril helix shown in Figure 1A. This coiled artificial muscle keeps its shape when dried, and when moisture is applied, this newly formed helical geometry will translate the untwisting/retwisting of twisted yarn to a uniaxial length change of the coiled muscle (Figure 1C), similar to the contraction and expansion found in plant tendrils. Unlike the single helix mechanism of well-known highly-oriented twisted artificial muscle fibers,[7a] the currently developed muscle yarn exhibits multihelix deformation[7b] initiated from the hierarchical assembly similar to helical plants. The geometry of the co-twisted hierarchical structures and the degree of volumetric change of the gel in the yarn's radial direction determine how much a multihelix yarn will untwist and change in length. The three helices—one in the microfilament unit (commercially placed when being drawn), one in the macroscale yarn body (placed by us during gel infusion), and one in the final coiled actuator—alter as a result of the volumetric change in the continuous gel phase. According to Figure 1D, the swelling of the hydrogel caused the co-twisted yarns to expand by a significant amount radially, which results in a significant contractile force acting through the coil axis. Large intercoil spaces enable the transformation of the generated force into contractile actuation.

Infusing hygroscopic materials within the microfilaments can also show significant challenges and operational limitations, as they should show both high moisture absorbance and 3D flexibility. Alginate hydrogel is a great candidate for high moisture absorbance but becomes highly brittle when dried,[15] and only coating the microfilaments with such material could cause premature filament-coating delamination. A secondary interfacial agent is therefore required that offers high dry-state flexibility and strongly binds alginate onto the filaments. Here, we precoated the individual microfilaments with highly robust elastomeric polyurethane (PU) hydrogel and further infused alginate (Alg) hydrogel both within interfilament spaces and onto the yarn surface, producing Alg-PU/yarn. Pre-coating of elastomeric hydrogel gave a high degree of interfacial adhesion between microfilaments and alginate, also providing torsional deformation flexibility without delaminating alginate gel from the microfilament surface. Mechanical torsion-assisted twisting and coiling of the yarns transformed them into hierarchical microstructures similar to those found in plant tendrils. Upon introducing moisture, these yarns can act as contractile artificial muscles (Alg-PU/yarn muscle) given the moisture-absorbed volumetric expansion of the alginate hydrogel. While moisture-activated artificial muscles are of the highest energy efficiency, their application in smart textile and soft robotic fields could be limited due to slow responses. As temperature-responsive polymeric artificial muscles can provide fast real-time actuation, we therefore treated our moisture-responsive yarn muscle by immersing within a buffer solution containing thermoresponsive poly(*N*-isopropylacrylamide) (NIPAM) monomer, producing temperature-sensitive gel structures, and tested their actuation performance while applying hydrothermal temperature fluctuations. The reversible hydration and dehydration of NIPAM via temperature change cause hydrophilic and hydrophobic phase transition behavior at lower critical solution temperature (LCST) of ≈32–34 °C,[16] which assists the faster actuation of our coiled yarn artificial muscles. This self-adaptive hydrothermal actuation of artificial muscle effectively mimics the inherited hydrotropism and thermotropism of plant tendrils. With actuating functionalities similar to natural plants, the developed artificial muscle from this study has the potential to perform on-demand autonomous works in variable environmental conditions.

2. Results and Discussion

2.1. Micromorphology and Mechanical Compliance

The surface morphology of the yarns and artificial muscles in dry state was initially characterized by using scanning electron microscopy (SEM) and relevant microanalysis was linked to their inherent mechanical properties evaluated from tensile testing. The practical utility of artificial muscles is highly dependent on the tensile properties of their precursor yarns, determining the feasibility of fabricated muscles as the building blocks of smart and sturdy devices and configurations.[17]

Figure 2A,B shows the surface morphology and relevant tensile stress-strain graphs of the yarns at different muscle fabrication stages. As-received textile cotton yarn is bulky unless stressed and consists of hundreds of microfilaments of ≈15 μm diameter. The ultimate tensile strength (UTS) of this yarn was evaluated to be ≈3.4 MPa while the yarn started to be permanently stretched at ≈7.5% tensile strain, before breaking. Coating with PU hydrogel increased the UTS of the yarn by

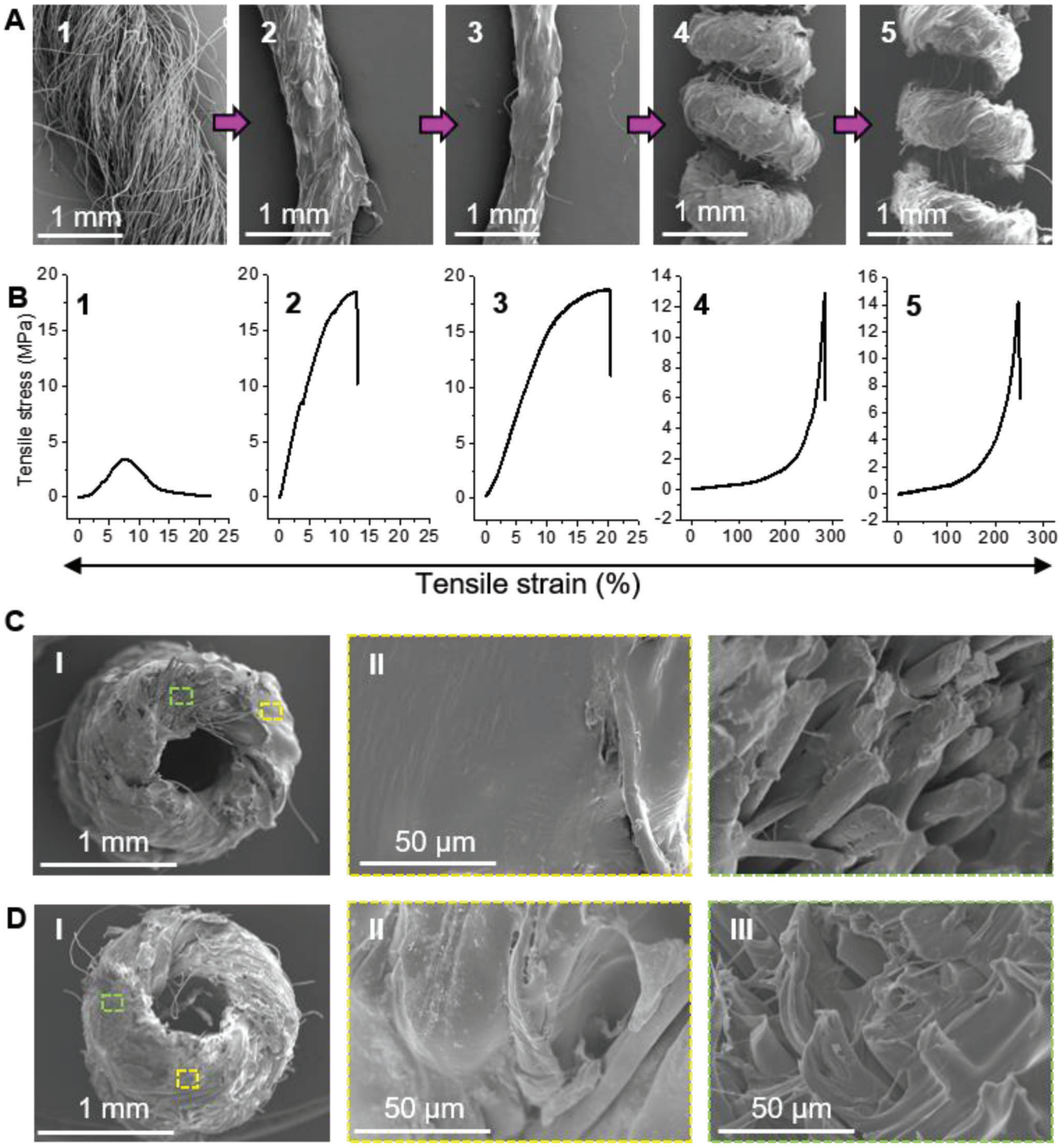

Figure 2. Microscopy images and relevant tensile properties of hierarchical hydrogel/textile yarn artificial muscles. A,B) Surface morphology and relevant tensile stress–strain graphs: 1) as-received textile cotton yarn, 2) PU gel impregnated yarn (PU/yarn), 3) alginate-coated PU/yarn (Alg-PU/yarn), 4) helically wound coiled Alg-PU/yarn muscle, and 5) NIPAM-treated thermoresponsive Alg-PU/yarn muscle. C) Cross-section morphology of an Alg-PU/yarn muscle; Sectioned: A free-standing muscle yarn, Surface: Uniform alginate coating over a surface portion, and Interface: Impregnated PU and alginate gel within the helical core with significant filament–filament spacings. D) Cross-section morphology of a NIPAM-treated thermoresponsive Alg-PU/yarn muscle; Sectioned: A free-standing muscle yarn, Surface: Uniform NIPAM treated alginate coating over a surface portion, and Interface: Polymerized NIPAM filling the gaps of impregnated PU and alginate gel within the helical core.

≈4.9 times, while also the twisting made the yarn cylindrical shaped and gave ≈2.5 times increase in tensile strain before breaking. High stretchability and mechanical durability of actuating yarns are essential when they are considered for wearable devices or smart textiles of such kind. Infusing alginate within PU-coated wet yarn and further twisting the yarn, herein called Alg-PU/yarn, gave more tensile flexibility, providing ≈2.7 times increase in ultimate tensile strain than that of as-received cotton yarn.

The highly twisted yarn was then wound around a mandrel to create the desired coiled Alg-PU/yarn muscle. Due to the large helix distance from the coil axis, mandrel-made coiled muscles have a limited stress tolerance ability, but they also have a very high degree of flexibility and stretchability, which is essential for configuring them for smart devices.[12a,18] Stretching our mandrel-coiled muscle also produced a perversion before the permanent coil distortion, much like the perversion in a plant tendril (Figure 1A). This has further established the microstructural resemblance between our artificial muscle and plant tendrils. The coiled muscle demonstrated exceptional structural robustness by withstanding a tensile strain of about 300% prior to the formation of a perversion. Treatment of the Alg-PU/yarn muscle with thermoresponsive NIPAM solution resulted in a 30% reduction in ultimate tensile strain while only marginally increasing the tensile stiffness (due to the higher modulus of NIPAM). The endurance of the yarn muscles was also assessed by putting them under cyclic tensile stress and found suitable for long-term use (detailed in Figure S7, Supporting Information). The yarn muscles withstood the test and retained the same shape they had when they were first fabricated.

Figure 2C,D shows the cross-sectionally taken SEM images of untreated and NIPAM-treated Alg-PU/yarn muscles, showing the uniformity of hollow cylindrical shape. High-magnification images revealed the morphology of gel-incorporated microfilaments within a twisted macroscale yarn. Decreasing strain value of the NIPAM-treated yarn muscle could also be attributed to the absence of interfilament spacings (Figure 2D) that were found from untreated Alg-PU/yarn muscle (Figure 2C). Prolonged immersion of the yarn muscle in NIPAM monomer containing buffer solution, polymerized NIPAM which filled the interfilament spacings. Interfilament spacings would allow uninterrupted hydrogel swelling and expansion when moisture is introduced, hence could offer a larger actuation strain. Therefore, we expect that the moisture-driven linear actuation of the untreated yarn muscle will be larger compared to that of hydrothermally induced NIPAM-treated ones. Both NIPAM-treated and untreated yarns have uniform surface coating while also showing insignificant number of exposed microfilaments (Figure 2C,D). It is worth noting that the exposed filaments are still gel coated onto their surface (interfacial elemental analysis provided in Figure S1, Supporting Information), maintaining the microstructure similar to the plant tendrils, and contributing to the volumetric expansion based linear actuation of the yarn muscles. Overall, the microscopic analysis and tensile properties suggest that the helically configured yarn muscles could provide large and reversible actuation stroke, given their wide and recoverable elastic strain range and large intercoil spacings.

2.2. Moisture Activated Actuation

Most natural resources are abundant and water is amongst the popular ones. Plants utilize water amongst others for the inherent triggering of shape deformation, that is, hydrotropism. The process is slow but energy-efficient, further including shape recovery using sunlight-induced hydrothermal tropism. Our microstructurally mimicked artificial muscles also mimic helical plant's actuating mechanism by using active moisture stimulus for shape deformation and passive hydrothermal stimulus for recovery.

Dynamic actuation output is the most suitable way to evaluate the real-time performance of artificial muscles, hence we first measured the time-based linear contraction and expansion of our Alg-PU/yarn muscle upon moisture stimulation. The initial observation was made upon adding water droplets onto a free, vertically suspended yarn muscle (while keeping the yarn end torsionally blocked) and optically recording the length change, and the reverse stroke was attained by passive drying under normal atmosphere as commonly experienced by plants. **Figure 3**A shows the results of moisture-stimulated linear actuation of the coiled Alg-PU/yarn muscle. While reversible actuation is mandated for all smart applications, it is also crucial to perform a few pre-conditioning actuation cycles for such twisted and coiled artificial muscles. Mechanical torsion guided twisted structures are subject to stress relaxation, both time-based free relaxation and external stimuli or stress-assisted relaxation.[19] Pre-conditioning (training) these helical structures will allow to release the residual temporary stresses that are not recoverable or reversible. We trained our Alg-PU/yarn muscle for three consecutive wetting/drying cycles when slight permanent stretching of muscle was noticed. In the fourth cycle and thereof, we observed a fully reversible, huge contraction strain of ≈24.5% (±0.5%) obtained within 6 min of introducing moisture (Figure 3A) (repeatability of actuation was also tested for 50 cycles, see Figure S8, Supporting Information).

The concept of moisture-driven linear actuation of this hydrogel-filled twisted and coiled yarn muscle is dependent on the volumetric expansion and contraction of the infused hygroscopic gel materials when hydrated and dried, respectively (Figure 3B). Since the helical structure is initially set by the infused and dried gel materials, this contraction/expansion usually causes a partial untwisting/retwisting of twisted yarn actuators that is free to rotate. As in the linear actuation test set-up, the yarn actuator was torsionally blocked at both ends and thus exhibited a length contraction/expansion, as demonstrated in the helix model of twisted/coiled artificial muscles. While Figure 3B partially images the change of macroscopic volume and length of an unloaded actuator, applying a controlled and constant stress to the dry actuator that controllably increases the coil bias angle provides a much higher actuation strain than the unloaded ones. For instance, hanging a ≈12 times heavier object from the actuator gave ≈50% contraction strain in <20 s when the actuator was fully swollen (Video S1, Supporting Information). We further evaluated the actuation capability of the actuator while lifting a ≈24 times heavier object and obtained a partial contraction of ≈33% of the initial length (Video S2, Supporting Information). The

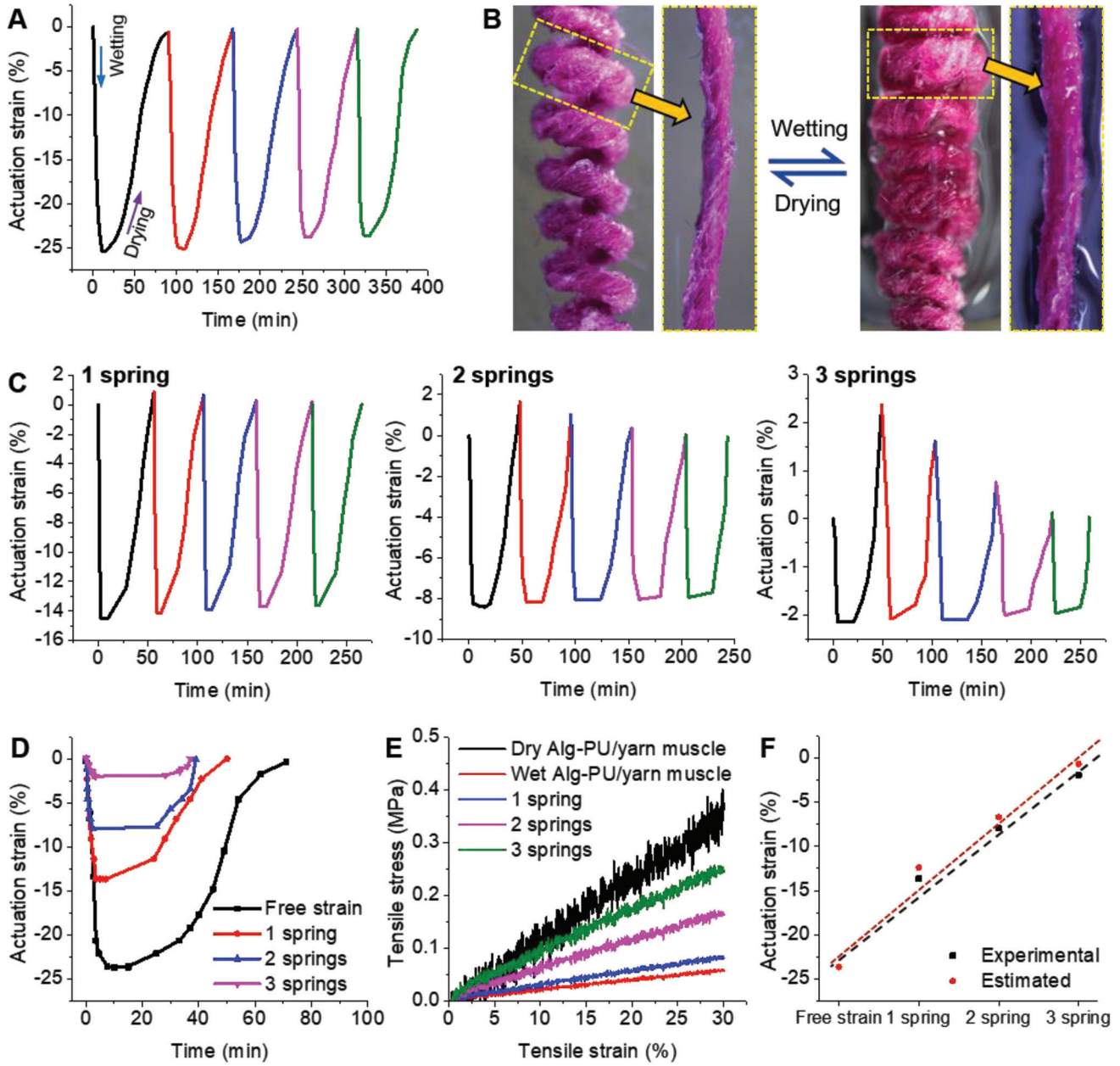

Figure 3. A) Moisture-activated actuation strain of a freely contracting Alg-PU/yarn muscle. B) Optical microscopy images show the coils of the muscle reversibly collapse and produce contractile actuation when moisture-activated, due to the radial expansion of the helically directed yarn. C) Moisture-activated actuation strain of a Alg-PU/yarn muscle when operated against different number of return springs. D) Comparison of actuation strains obtained under different mechanical conditions for one actuation cycle (fifth cycle considered in this case). E) Stress–strain curves of different numbers of springs and a Alg-PU/yarn muscle in dry and wet conditions. F) Validation of experimental results with theoretically estimated actuation results.

decrease of actuation strain with increasing stress in the uniaxial direction is analogous to the actuation mechanics of stretchable artificial muscles which represent a mix of actuation-generated force and stroke.[20]

Next, we assessed the performance of actuating yarns when integrated within smart systems that apply variable stresses over time. In these cases, the actuating muscle yarns are attached to other passive yarns (such as in smart textile fabrics), while both ends are tethered and actuating strains are measured at the junction. A benefit of the both-end-tethered configuration is the ability to fix the location of actuating yarn, while the free end of the single-end-tethered system can move in any direction and has limited practical utility. The assessment of the feasibility of our yarn muscle in such an integrated system can be performed via testing the yarn against variable stresses applied by series-connected elastic and non-actuated return springs. This investigation also allows the assessment of resistance by the artificial muscle against the tensile stresses that could permanently

distort the coiled structure. We here applied three different tensile stresses by using 1, 2, and 3 spandex return springs that linearly scale the extents of oppositely applying forces to the direction of muscle contraction and measured the contraction strain (Figure 3C). Against 1 spring, our moisture-responsive muscle provided ≈14% (±1%) reversible contraction strain. While the actuation strain was decreased, it is worth noting that the full reversibility from this experiment was obtained from the very first actuation cycle, providing better practical feasibility of the developed muscle. We further evaluated the actuation strains of the developed muscle against 2 and 3 springs, producing gradually less contraction strains in relevant first cycles with higher expansion. Comparative actuation results from fully reversible cycles are shown in Figure 3D along with free strains. The decreasing trend is obvious as an increasing number of springs applied higher opposing stress to the contraction strains while assisting the expansion strains by pulling back. For the general case where the actuating muscle fiber is operated against a return spring of tensile stiffness E_{spring}, the contraction strain ($\Delta\epsilon$) at the junction between artificial muscle and return spring can be determined from the variable force balance equation:

$$\Delta\epsilon = \Delta\epsilon_{free} + E_{spring}\left(\frac{1}{E'_{muscle}} - \frac{1}{E_{muscle}}\right) \quad (1)$$

where $\Delta\epsilon_{free}$ is the actuation strain obtained from a freely operated muscle (as shown in Figure 3A) and E'_{muscle} and E_{muscle} are the tensile stiffnesses of the yarn muscle in actuated (wet) and non-actuated (dry) states, respectively. The tensile stiffnesses were calculated from the slope of stress-stress curves (Figure 3E) obtained from tensile tensing of relevant yarns. This equation provides a basis for theoretically estimating the actuation strain of a yarn muscle against variable stress conditions, provided that the free actuation strain is known. Figure 3F shows the comparison of theoretical estimations and experimental measurements of relevant systems, which shows good agreement with each other. Therefore, the developed moisture-responsive Alg-PU/yarn muscle is of high controllability and scalability, and suitable for conditions with variable stress conditions hence smart wearable configurations.

2.3. Thermoresponsive Actuation

Hydrogel swelling assisted by moisture absorption is dependent on the balance of the osmotic forces that extend the polymer network and the contrasting elastic forces obtained from the extended polymer segments and the surrounding humidity. Similar to the natural moisture absorption and hydrotropism of helical plants, the artificial and passive actuation process from moisture-absorbed hydrogels is also slow, like 6 min for contraction and 70 min for expansion (Figure 3). Passive responsiveness is also varied depending on the moisture content of ambient atmosphere; for instance, the passive return that we performed in tropical Asia-Pacific summer will be faster in a dry environment such as in Northern-European winter or American desert). This slow responsiveness also makes our developed moisture-responsive Alg-PU/yarn muscle only suitable for limited systems whose primary focus is energy efficiency or untethered, autonomous response. Hence, there is a need of making artificial systems that are both energy efficient and fast, also inheriting the adaptive hydrotropism feature.

In order to make the actuation even faster, the Alg-PU/yarn muscle was treated with a buffer solution consisting of thermoresponsive NIPAM polymer. NIPAM is an amphiphilic polymer consisting of hydrophilic (amide) and hydrophobic (isopropyl) groups, and its fast moisture absorption/desorption-driven actuation is controlled by surrounding media passing lower critical solution temperature (LCST) of ≈32–34 °C.[16] It was anticipated that treating our Alg-PU/yarn muscle with NIPAM would give a similar fast actuation strain rate of the coiled structures. To investigate the potential for thermoresponsive actuation, NIPAM-treated Alg-PU/yarn muscle was tested for five cycles at different temperatures above and below the transition region (repeatability of actuation was also tested for 50 cycles, see Figure S8, Supporting Information). For instance, when activated by passing hot water of ≈47 °C, it expanded rapidly and reached a maximum strain of ≈16.2% (±1%). When cold water of ≈7 °C that is below LCST was passed, the yarn muscle was contracted proving full recovery of actuation strain (**Figure 4**A). The process was extremely fast, providing >15% expansion in <3 s (Figure 4B). The contraction till full recovery (≈15%) was a bit slower, taking ≈12 s. Figure 4C shows the optical microscopy images of a yarn muscle undergoing thermoresponsive actuation, where infrared images from a thermal imager show the upper and lower temperature limits. The strain rate was also calculated from the gradient of the first linear part of the actuation profile during the first part of both expansion and contraction cycles,[11a,21] this typically being within the first few seconds after introducing hot and cold water, respectively. The average strain rate for all five thermoresponsive actuation cycles was found to be ≈5.2% s^{-1} at muscle expansion and ≈3.1% s^{-1} at muscle contraction, which is the fastest amongst previously reported hydrogel-based linear actuators.[22] While hydrogel actuators are promising technology for soft robotics and other biomimetic technologies, the slow actuating nature hinders their application potentiality. Enhancing the actuation speed is one of the key considerations in the research field of stimuli-responsive hydrogels. Table 1 compares the actuation speed of our developed hydrogel artificial muscles with the similar ones presently available.

The thermoresponsive actuation of NIPAM-treated Alg-PU/yarn muscle effectively mimics the temperature-dependent change of hydrotropism in plant tendrils, also replicating their inherited thermotropism. In the artificial muscle, water temperature above LCST causes conformation of NIPAM chain whose hydrophilic amide groups were buried by hydrophobic isopropyl groups, which resulted in releasing a significant amount of water. While at temperatures lower than LCST, the hydrophilic amide groups of NIPAM chain expose and rehydration occurs of the NIPAM-treated alginate hydrogel (Figure 4D). These volumetric conformational changes drive the linear actuation of coiled yarn muscle by following a similar mechanism related to untwisting and retwisting of Alg-PU/yarn muscle when water is absorbed and released, respectively. Video S3, Supporting Information, shows the macroscopic volume change of an example Alg-PU/yarn muscle undergoing rapid hydrothermal contraction and expansion when partially exposed to cold and hot water, respectively. Video S4, Supporting Information, shows the overall hydrothermal actuation of a full-length yarn muscle when

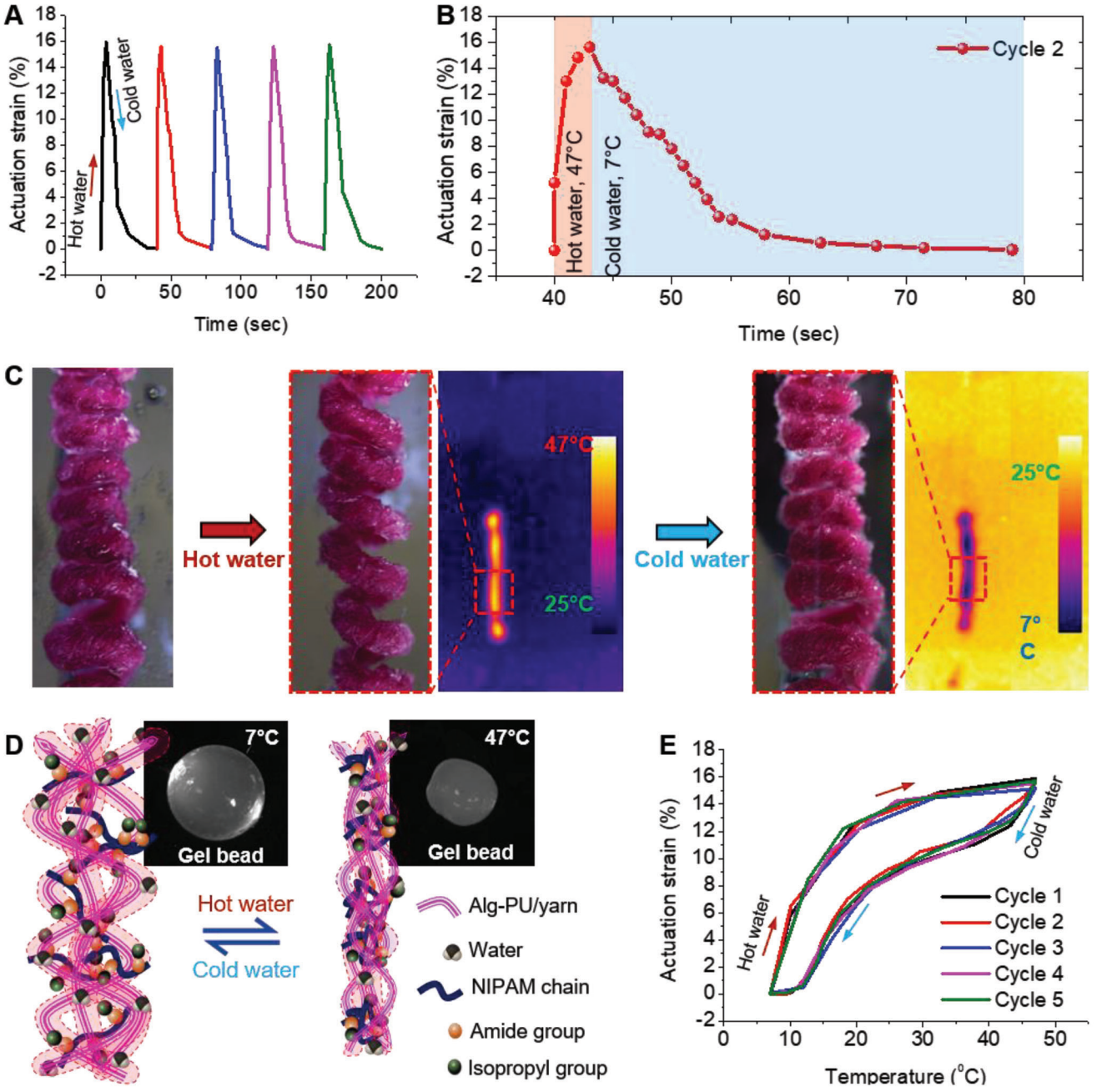

Figure 4. Thermoresponsive actuation of NIPAM treated Alg-PU/yarn muscle. A) Time-based actuation strain for five consecutive heat/cool cycles. B) Descriptive image showing how fast the heating activates the muscle. C) Optical microscopy images of a yarn muscle showing thermoresponsive actuation and infrared images showing the upper and lower temperature limits. D) Schematic illustration of deswelling/swelling of a thermally activated NIPAM-treated Alg-PU/yarn with inset showing the thermally triggered volume change of an example bead prepared with PNIPAM-treated alginate. E) Five consecutive cycles of reversible actuation based on temperature fluctuation.

volumetrically stimulated. The actuator was able to show ≈23% length expansion in ≈4 s when hot water was applied, as well as >90% reverse stroke in <7 s with cold water. A slight hysteretic behavior was observed for systematic expansion and contraction cycles, mostly due to the heat difference in heat transfer rate triggered by hot and cold water. It is worth noting that the temperature shown here is the surface temperature of the yarn muscle sensed by the thermal imaging camera.

2.4. Yarn Washability and Environmental Adaptability

Good surface coverage of gel material is important for real-world applications of yarn muscles, and this is expected that the developed yarn muscles will have appropriate gel-filament adhesion that remains undamaged during abrasion or other mechanical shearing such as during washing of gel-incorporated yarns. To mimic this, we tested the degree of gel-filament adhesion

Table 1. Comparative actuation speed of hydrogel-based linear artificial muscles..

Actuator materials	Actuator shape	Stimulus	Best speed [% s^{-1}]	
			Expansion	Contraction
This work: Thermoresponsive hydrogel-infused textile yarn	Helical (mandrel made coils)	Hydrothermal	≈5.2%	≈3.1%
Electrospun poly(acrylic acid) yarn; ref. [1a]	Helical (co-twisted multifilament)	pH, moisture	≈0.177	≈2.45
Polyacrylamide, incorporated with cellulose nanocrystals; ref. [22a]	Helical (homo- and heterochiral coils)	Moisture	≈1.624	≈3.251
Alginate beads, treated with NIPAMs; ref. [22b]	Cylindrical (McKibben type)	Hydrothermal	≈0.001	≈0.011
Poly(acrylic acid), poly(methyl methacrylate); ref. [22c]	Cylindrical (McKibben type)	pH	≈0.002	≈0.002
Poly(acrylic acid), incorporated with hydrophilic PU ref. [23]	Cylindrical (rod type)	Light, pH	Not reported	≈0.044
Polyacrylamide, polymerized with poly(acrylic acid); ref. [24]	Flat bar (ribbon type)	UV light	Not reported	≈0.017
Anionic polyacrylonitrile, mixed with cellulose fibers; ref. [25]	Cylinder (solid fiber)	Moisture	≈1.62	≈0.95
Polyaniline-based conducting hydrogel; ref. [26]	Rectangular bar	Electrochemical	≈0.75	≈0.75
NIPAM-infused carbon nanotube yarn; ref. [27]	Cylinder (Multifilament yarn)	Glucose	Not reported	≈0.001
Monofilament nylon fiber, coated with phenylboronic acid containing polyacrylamide; ref. [28]	Cylinder (core–shell fiber)	Glucose	≈0.036	≈0.038
Sodium alginate, infused with a liquid electrolyte; ref. [29]	Flat rectangular bar	Electrochemical	≈0.002	Not reported
Poly(vinyl alcohol), hybridized with ferritin nanoparticles; ref. [30]	Nanofibrous mat	pH	≈0.001	≈0.001
Poly(acrylic acid), doped with calcium ion; ref. [31]	Rectangular strip	Hydrothermal	Not reported	0.065

after employing wet washing of a gel-incorporated yarn (Alg-PU/yarn). The yarn was initially placed within a mesh washing bag that is typically used to wash delicate garments. Then, the yarn-containing bag was placed in a front loader household washing machine and washed for 20 min in ≈40 °C water. It is worth noting that the use of detergent would not be necessary for washing such gel-incorporated yarns, as the swollen gel would open up their pores and their cyclic motions within the washer will expel the dirt or contaminates. **Figure 5**A shows the microscopy images of the Alg-PU/yarn both before and after washing. Figure 5A-I shows the optical image of the yarn before washing, where the magnified SEM image shows excellent gel coverage on the yarn surface. Figure 5A-II shows the yarn after washing, while still in wet condition. When dried, the washed yarns showed well-persisted gel coverage onto the yarn surface with no hint of gel delamination (Figure 5A-III). It is worth noting that our gels are not cross-linked, making them less brittle when in a dry condition. The gel coverage on individual filaments was also microscopically studied after yarn washing (Figure 5B). As desired, interfilament gel content was well preserved after the wash which critically confirmed that Alg-PU/yarn can effectively be used as the building block of reusable smart devices.

It is also desired from reusable smart devices that comprise artificial muscle yarns that they offer fairly consistent autonomous actuation over the lifetime. Tropisms in helical plants allow them to respond to environmental changes and repetitively deform themselves to fit the changed conditions. Our current study is nature-inspired, and smart and autonomous operation in an energy-efficient manner is the ultimate objective of our Alg-PU/yarn muscles. To show the responsiveness to environmental stimuli and triggering of a smart and autonomous function, we here build a prototype window shutter incorporating the developed Alg-PU/yarn muscle (Figure 5C). The aim was to show autonomous closing of the shutter when environmental moisture content goes extremely high, that is, when raining. Video S5, Supporting Information, shows the top view of how the moisture-induced contraction of the yarn muscle closes the window shutter. The movable shutter is hung in favor of the gravity and the closing process acts opposite to the direction of gravity. The moisture-responsive yarn muscle was quick enough to respond to the wet environment, almost fully closing the shutter in less than 70 s. This is one smart yet practical example that our yarn muscles can be used for. Our gel-incorporated yarn muscles can be produced in an automated, continuous manner such as in a textile processing industry that would enable the production of kilometer-long actuating yarns, providing good future prospects of high-volume practical utility.[32] The production of the batches of actuating yarn and coiled muscle is elaborated in Figure S6, Supporting Information. As for heavy and multidimensional actuating applications, yarn muscles can be configured into fabrics with varied geometry to fit the actual requirements.[33]

3. Conclusion

Helically shaped plants have a hierarchy of microstructural chirality with the helices of cellulose fibrils, and upon moisture

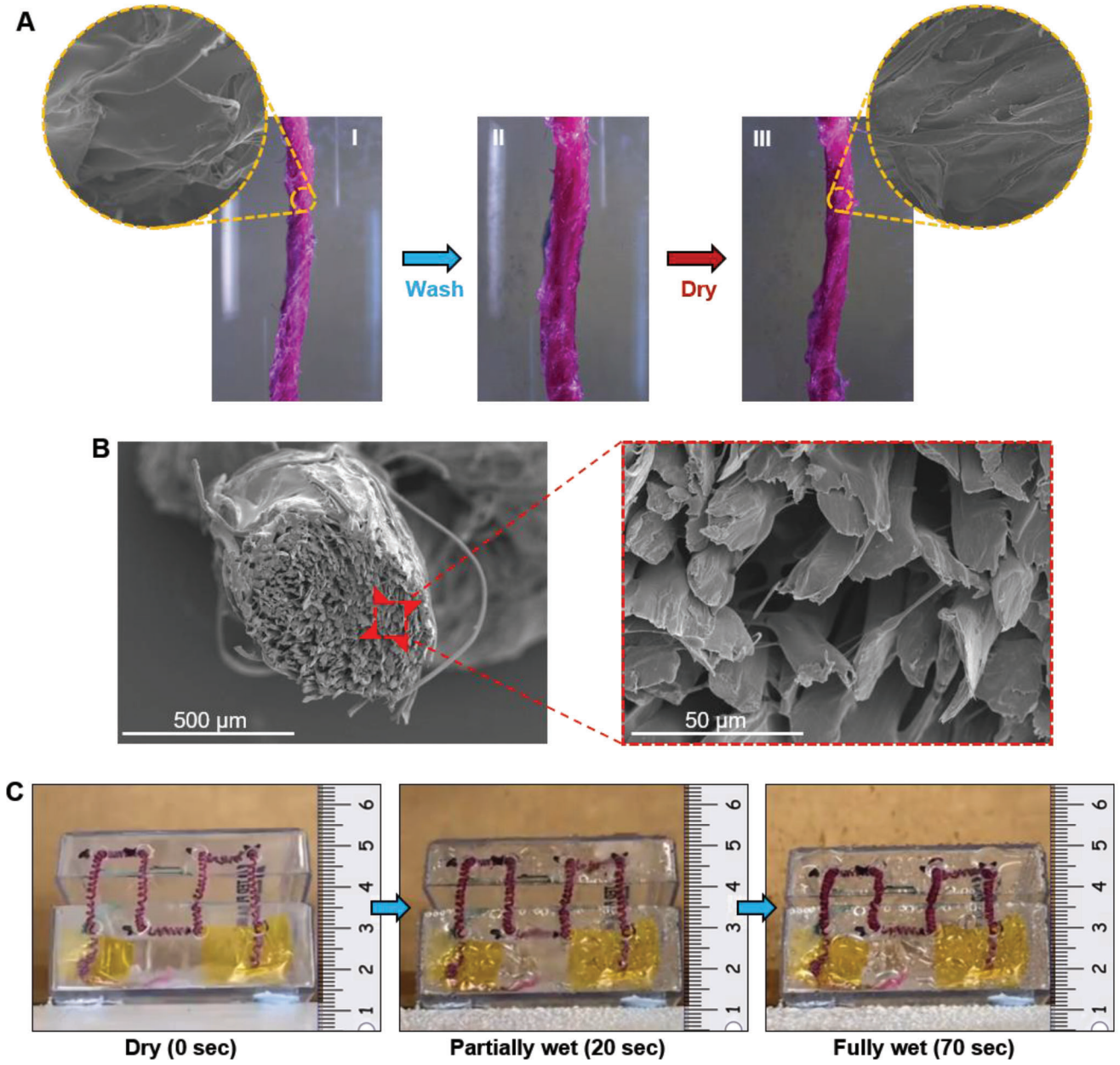

Figure 5. Washability of Alg-PU/yarn and example applicability of the coiled yarn muscle. A) Microscopy images of the yarn before and after washing. B) Persisted interfilament gel after yarn washing. C) A prototype autonomous window with integrated coiled Alg-PU/yarn muscle being closed when water mist is introduced.

and heat-induced volume change, these fibrils produce torsion that eventually triggers uniaxial length change of the overall system. The humidity and temperature responsiveness of such plants are typically known as hydrotropism and thermotropism, respectively. We here demonstrate that the (micro-) functionalities of hydrotropism and thermotropism of helical plants can be achieved by using microstructural mimicking, providing the "artificial muscle with natural intelligence". The morphing process used low-cost materials, incorporating hydrogel-infused hierarchically patterned helically wound multifilament yarns, producing coiled-shaped hierarchical artificial muscles. Fully reversible free contraction strain of ≈24.5% was obtained by introducing moisture, showing the effectiveness of microstructural mimicking of helical plants while replicating their hydrotropism in artificial materials. Treating this coiled actuator with a thermoresponsive gel solution produced temperature-responsive artificial muscles providing >15% actuation strain in <3 s or a strain rate of 5.2% s^{-1}, which is the fastest amongst hydrogel-based linear actuators reported so far. Rapid and large actuation stroke resulted from the multihelix deformation originating from the hierarchical yarn structure with microfilaments, similar to moisture-induced microfibrils deformation of helical

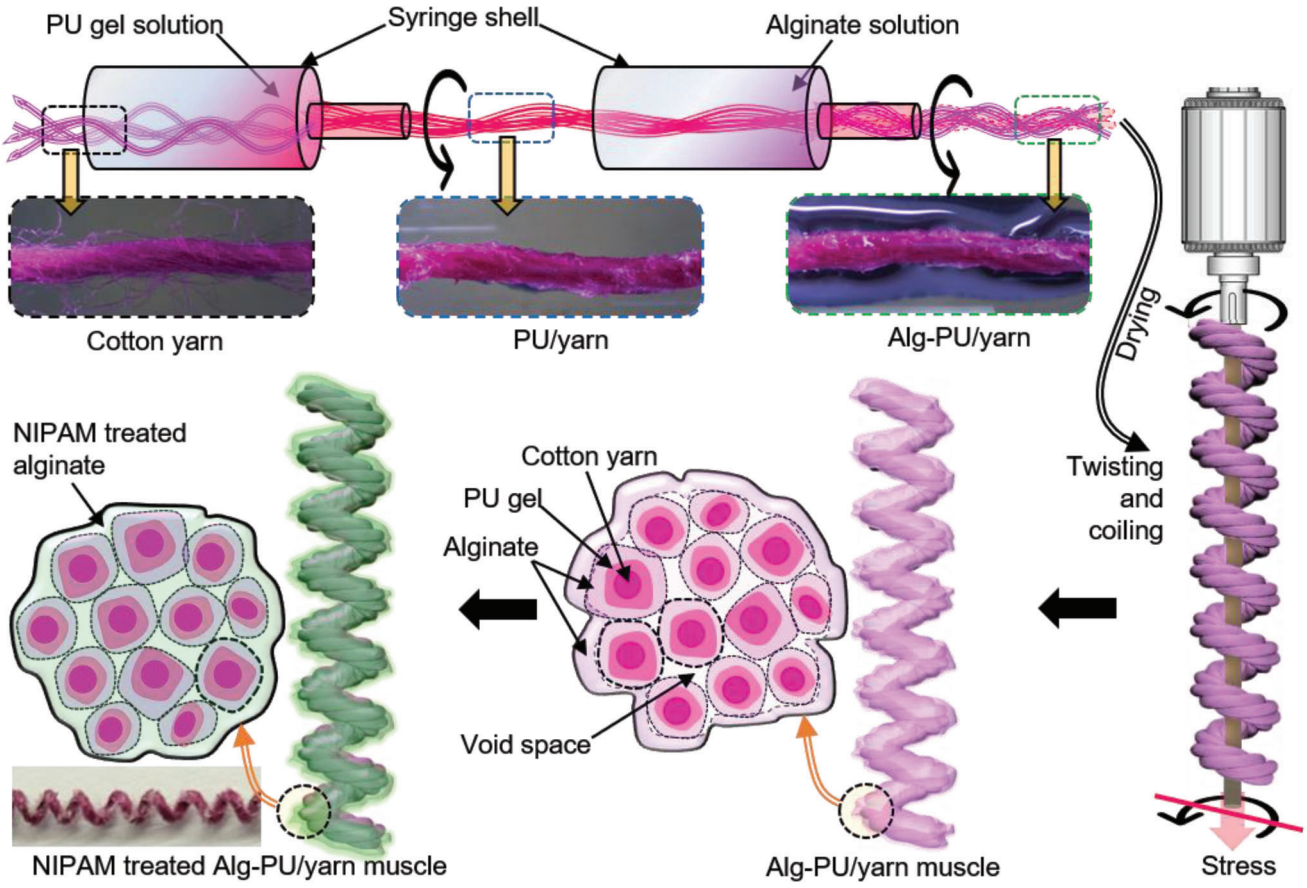

Figure 6. Summary method illustration of fabricating hierarchical artificial muscle.

plants. This thermoresponsive actuation effectively mimics the thermotropism, that is, temperature-dependent change of inherited hydrotropism, in plant tendrils at their microfibril level. We further demonstrated a prototype autonomous window shutter, utilizing the developed artificial muscle for autonomous and self-adaptive actuation in response to the external humidity change. Having a filament-gel interface-strengthening material, the developed artificial muscle is highly durable and washable, making them suitable for creating long-lasting and reusable smart devices.

4. Experimental Section

Fabrication Method of Yarn Muscle: The PU hydrogel was made using commercially sourced granules of ether-based hydrophilic urethanes (AdvanSource Biomaterials Corporation, MS, USA) and the preparation method is described in Figure S3, Supporting Information. A summary method illustration of the fabrication of yarn muscle is demonstrated in **Figure 6**. Initially, the gel solution was suctioned into a syringe and as-received cotton yarn was passed through the solution followed by twist drawing the gel-containing yarn through the syringe tip. Concurrent partial twisting of the yarn while drawing allowed the uniform diffusion of gel material within the interfilament spacings of the yarn. The yarn was then diffused with alginate (Alg) solution following a similar drawing and partial twisting process through another syringe that was filled with alginate solution. The prepared Alg-PU/yarn was dried for 1 h under normal atmosphere. The dried yarn was further twisted onto the onset of coiling by vertically suspending from an electric motor and spooled for further use (a batch of yarn is shown in Figure S6, Supporting Information). This highly twisted yarn was then helically deformed via wrapping around a metal mandrel followed by drying in an oven to obtain the desired hierarchical coiled Alg-PU/yarn artificial muscle (details in Figures S3 and S6, Supporting Information). Alg-PU/yarn muscle was then given thermoresponsive actuation property by treating the yarn in a buffer solution containing NIPAM monomer. The preparations of NIPAM buffer solution are detailed in Figure S4, Supporting Information. NIPAM was infused along the helices of the coiled actuator while still maintaining the helical geometry and creating a thermoresponsive actuator with a substantial intercoil gap.

While the current research provides the proof-of-concept for the realization of plant tropism in biomimetic artificial materials, additional improvement on scalable preparation was required. By the analogy of twisted and coiled yarn actuators, the currently developed artificial muscle will alter actuation performance based upon the yarn diameter, number of inserted twists, and change in gel volume when stimulated. These parameters should be optimized for achieving controlled actuation, and it was suggested to develop a performance predictive model that will estimate the actuation strain and force generation based upon fabrication parameters. Such a theoretical approach will assist in preparing actuators on a larger scale with the desired actuation capabilities.

Characterization Procedure: The macrostructure of the precursor yarn and fabricated artificial muscles were evaluated using an optical microscope (Olympus BX51, Tokyo, Japan). Video S3, Supporting Information, was recorded using the same optical microscope. The surface and interface morphology of the yarn muscles in dry state were studied via SEM

(Hitachi SU3500, Tokyo, Japan) using 5 keV accelerated voltage. Real-time temperature sensing of the thermoresponsive actuator was recorded using an infrared thermal imaging camera (RS700, RS Components Pty Ltd, NSW, Australia). A universal mechanical tester (Instron 5584, MA, USA) was used to measure the tensile properties of the yarn muscles under 5 mm min^{-1} strain rate.

Actuation Test: Fabricated coiled yarn muscles were vertically suspended from a sturdy hanger with top-end fixed in both tensile and torsional context. For free actuation test, the coiled yarn muscle was loaded with a lightweight horizontally suspended rod that kept the muscle straight and torsionally blocked at the free end. Actuators with return spring attachment were tested similarly while measuring the actuation strain at the junction of the actuating yarn and return spring. The detailed actuation test method is given in Figure S5, Supporting Information. Both moisture and hydrothermally driven actuation was optically recorded (OPTEK Digital Microscope Camera, ISSCO Australia) and the actuation strain was measured using the ImageJ image processing program.

Supporting Information

Supporting Information is available from the Wiley Online Library or from the author.

Acknowledgements

S.A. and Z.Z. thank the support from Australian Research Council Linkage Project LP200100403 and Discovery Project DP200101397. E.W.H.J acknowledges financial support from the Swedish Government Strategic Research Area in Materials Science on Functional Materials at Linköping University (Faculty Grant SFOMatLiU No. 2009 00971) and Erling-Persson Family Foundation (No. 2020-0054).

Open access publishing facilitated by The University of Queensland, as part of the Wiley - The University of Queensland agreement via the Council of Australian University Librarians.

Conflict of Interest

The authors declare no conflict of interest.

Author Contributions

S.A., E.W.H.J., and Z.Z. conceived and supervised the project. S.A., X.Z., and B.S. designed and performed the experimental measurements. S.A., X.Z., S.N., and B.S. performed the data analysis. S.A., X.Z., S.N., B.S., E.W.H.J., and Z.Z. wrote the manuscript.

Data Availability Statement

The data that support the findings of this study are available from the corresponding author upon reasonable request.

Keywords

artificial muscles, biomimicked technology, hydrogels, smart devices, soft actuators, soft robotics, textile yarns

Received: December 22, 2022
Revised: March 15, 2023
Published online:

[1] a) G. M. Spinks, N. D. Martino, S. Naficy, D. J. Shepherd, J. Foroughi, *Sci. Rob.* **2021**, *6*, eabf4788; b) I. Must, E. Sinibaldi, B. Mazzolai, *Nat. Commun.* **2019**, *10*, 344.

[2] a) D. J. Shepherd, G. M. Spinks, *Adv. Mater. Technol.* **2019**, *4*, 1800525; b) M. Kanik, S. Orguc, G. Varnavides, J. Kim, T. Benavides, D. Gonzalez, T. Akintilo, C. C. Tasan, A. P. Chandrakasan, Y. Fink, P. Anikeeva, *Science* **2019**, *365*, 145; c) A. Kataruka, S. B. Hutchens, *Matter* **2021**, *4*, 3991.

[3] a) M. Shi, E. M. Yeatman, *Microsyst. Nanoeng.* **2021**, *7*, 95; b) M. D. Lima, M. W. Hussain, G. M. Spinks, S. Naficy, D. Hagenasr, J. S. Bykova, D. Tolly, R. H. Baughman, *Small* **2015**, *11*, 3113; c) S. H. Kim, C. H. Kwon, K. Park, T. J. Mun, X. Lepró, R. H. Baughman, G. M. Spinks, S. J. Kim, *Sci. Rep.* **2016**, *6*, 23016.

[4] a) D. Rus, M. T. Tolley, *Nature* **2015**, *521*, 467; b) C. Kaspar, B. J. Ravoo, W. G. van der Wiel, S. V. Wegner, W. H. P. Pernice, *Nature* **2021**, *594*, 345; c) Y. Chen, H. Zhao, J. Mao, P. Chirarattananon, E. F. Helbling, N.-S. P. Hyun, D. R. Clarke, R. J. Wood, *Nature* **2019**, *575*, 324.

[5] S. M. Mirvakili, I. W. Hunter, *Adv. Mater.* **2018**, *30*, 1704407.

[6] J.-S. Wang, G. Wang, X.-Q. Feng, T. Kitamura, Y.-L. Kang, S.-W. Yu, Q.-H. Qin, *Sci. Rep.* **2013**, *3*, 3102.

[7] a) J. Foroughi, G. Spinks, *Nanoscale Adv.* **2019**, *1*, 4592; b) P. Chen, Y. Xu, S. He, X. Sun, S. Pan, J. Deng, D. Chen, H. Peng, *Nat. Nanotechnol.* **2015**, *10*, 1077; c) J. Mu, M. Jung de Andrade, S. Fang, X. Wang, E. Gao, N. Li, H. Kim Shi, H. Wang, C. Hou, Q. Zhang, M. Zhu, D. Qian, H. Lu, D. Kongahage, S. Talebian, J. Foroughi, G. Spinks, H. Kim, H. Ware Taylor, J. Sim Hyeon, Y. Lee Dong, Y. Jang, J. Kim Seon, H. Baughman Ray, *Science* **2019**, *365*, 150.

[8] a) Q. Yang, J. Fan, G. Li, *Appl. Phys. Lett.* **2016**, *109*, 183701; b) Y. Cheng, R. Wang, K. H. Chan, X. Lu, J. Sun, G. W. Ho, *ACS Nano* **2018**, *12*, 3898; c) M. Wang, B.-P. Lin, H. Yang, *Nat. Commun.* **2016**, *7*, 13981.

[9] a) L. Huang, X. Xie, H. Huang, J. Zhu, J. Yu, Y. Wang, Z. Hu, *Sens. Actuators, A* **2020**, *302*, 111793; b) S. H. Kim, M. D. Lima, M. E. Kozlov, C. S. Haines, G. M. Spinks, S. Aziz, C. Choi, H. J. Sim, X. Wang, H. Lu, D. Qian, J. D. W. Madden, R. H. Baughman, S. J. Kim, *Energy Environ. Sci.* **2015**, *8*, 3336; c) J. v. d. Weijde, B. Smit, M. Fritschi, C. v. d. Kamp, H. Vallery, *IEEE. ASME. Trans. Mechatron.* **2017**, *22*, 1268.

[10] S. Aziz, B. Villacorta, S. Naficy, B. Salahuddin, S. Gao, T. A. Baigh, D. Sangian, Z. Zhu, *Appl. Mater. Today* **2021**, *23*, 101021.

[11] a) S. Aziz, J. G. Martinez, B. Salahuddin, N.-K. Persson, E. W. H. Jager, *Adv. Funct. Mater.* **2021**, *31*, 2008959; b) R. Aston, K. Sewell, T. Klein, G. Lawrie, L. Grøndahl, *Eur. Polym. J.* **2016**, *82*, 1.

[12] a) C. S. Haines, M. D. Lima, N. Li, G. M. Spinks, J. Foroughi, J. D. W. Madden, S. H. Kim, S. Fang, M. Jung de Andrade, F. Göktepe, Ö. Göktepe, S. M. Mirvakili, S. Naficy, X. Lepró, J. Oh, M. E. Kozlov, S. J. Kim, X. Xu, B. J. Swedlove, G. G. Wallace, R. H. Baughman, *Science* **2014**, *343*, 868; b) S. Aziz, S. Naficy, J. Foroughi, H. R. Brown, G. M. Spinks, *J. Polym. Sci., Part B: Polym. Phys.* **2016**, *54*, 1278.

[13] a) Y. Abraham, C. Tamburu, E. Klein, J. W. C. Dunlop, P. Fratzl, U. Raviv, R. Elbaum, *J. R. Soc., Interface* **2012**, *9*, 640; b) A. Paajanen, S. Ceccherini, T. Maloney, J. A. Ketoja, *Cellulose* **2019**, *26*, 5877; c) S. J. Gerbode, J. R. Puzey, A. G. McCormick, L. Mahadevan, *Science* **2012**, *337*, 1087.

[14] S. Aziz, J. G. Martinez, J. Foroughi, G. M. Spinks, E. W. H. Jager, *Macromol. Mater. Eng.* **2020**, *305*, 2000421.

[15] a) D. Cao, J. G. Martinez, E. S. Hara, E. W. H. Jager, *Adv. Mater.* **2022**, *34*, 2107345; b) K. Y. Lee, D. J. Mooney, *Prog. Polym. Sci.* **2012**, *37*, 106.

[16] a) Y. Akiyama, T. Okano, in *Switchable and Responsive Surfaces and Materials for Biomedical Applications*, (Ed: Z. Zhang), Woodhead Publishing, Oxford **2015**; b) L. Xiao, A. B. Isner, J. Z. Hilt, D. Bhattacharyya, *Appl. Polym. Sci.* **2013**, *128*, 1804.

[17] a) A. Maziz, A. Concas, A. Khaldi, J. Stålhand, N.-K. Persson, E. W. H. Jager, *Sci. Adv.* **2017**, *3*, e1600327; b) J. Foroughi, G. M. Spinks, S. Aziz, A. Mirabedini, A. Jeiranikhameneh, G. G. Wallace, M. E. Kozlov, R. H. Baughman, *ACS Nano* **2016**, *10*, 9129; c) S. Aziz, G. M. Spinks, *Mater. Horiz.* **2020**, *7*, 667.
[18] C. S. Haines, N. Li, G. M. Spinks, A. E. Aliev, J. Di, R. H. Baughman, *Proc. Natl. Acad. Sci. USA* **2016**, *113*, 11709.
[19] S. Aziz, S. Naficy, J. Foroughi, H. R. Brown, G. M. Spinks, *J. Appl. Polym. Sci.* **2017**, *134*, 45529.
[20] a) G. M. Spinks, *J. Mater. Res.* **2016**, *31*, 2917; b) S. Aziz, S. Naficy, J. Foroughi, H. R. Brown, G. M. Spinks, *Sens. Actuators, A* **2018**, *283*, 98.
[21] D. Melling, S. Wilson, E. W. H. Jager, *Smart Mater. Struct.* **2013**, *22*, 104021.
[22] a) Y. Cui, D. Li, C. Gong, C. Chang, *ACS Nano* **2021**, *15*, 13712; b) B. Salahuddin, H. Warren, G. M. Spinks, *Smart Mater. Struct.* **2020**, *29*, 055042; c) V. Mansard, *Soft Matter* **2021**, *17*, 9644.
[23] M. P. M. Dicker, A. B. Baker, R. J. Iredale, S. Naficy, I. P. Bond, C. F. J. Faul, J. M. Rossiter, G. M. Spinks, P. M. Weaver, *Sci. Rep.* **2017**, *7*, 9197.
[24] Y. Ma, M. Hua, S. Wu, Y. Du, X. Pei, X. Zhu, F. Zhou, X. He, *Sci. Adv.* **2020**, *6*, eabd2520.
[25] L. Mao, Y. Hu, Y. Piao, X. Chen, W. Xian, D. Piao, *Curr. Appl. Phys.* **2005**, *5*, 426.
[26] Z. Sun, L. Yang, J. Zhao, W. Song, *J. Electrochem. Soc.* **2020**, *167*, 047515.
[27] S.-H. Lee, T. H. Kim, M. D. Lima, R. H. Baughman, S. J. Kim, *Nanoscale* **2016**, *8*, 3248.
[28] H. J. Sim, Y. Jang, H. Kim, J. G. Choi, J. W. Park, D. Y. Lee, S. J. Kim, *ACS Appl. Mater. Interfaces* **2020**, *12*, 20228.
[29] J. Yang, Z. Wang, J. Yao, S. Wang, *Sens. Actuators, A* **2021**, *332*, 113126.
[30] M. K. Shin, G. M. Spinks, S. R. Shin, S. I. Kim, S. J. Kim, *Adv. Mater.* **2009**, *21*, 1712.
[31] L. Hua, C. Zhao, X. Guan, J. Lu, J. Zhang, *Sci. China Mater.* **2022**, *65*, 2274.
[32] C. Huniade, D. Melling, C. Vancaeyzeele, G. T.-M. Nguyen, F. Vidal, C. Plesse, E. W. H. Jager, T. Bashir, N.-K. Persson, *Adv. Mater. Technol.* **2022**, *7*, 2101692.
[33] N.-K. Persson, J. G. Martinez, Y. Zhong, A. Maziz, E. W. H. Jager, *Adv. Mater.* **2018**, *3*, 1700397.